Global impact of lightning-produced oxidants

Jingqiu Mao[1], Tianlang Zhao[1], Christoph A. Keller[2,3], Xuan Wang[4], Patrick J. McFarland[5], Jena M. Jenkins[5], William H. Brune[7]

[1]Department of Chemistry and Biochemistry and Geophysical Institute, University of Alaska, Fairbanks, Fairbanks, AK, USA.
[2]Universities Space Research Association, Columbia, MD, USA
[3]NASA Global Modeling and Assimilation Office, Goddard Space Flight Center, Greenbelt, MD, USA
[4]School of Energy and Environment, City University of Hong Kong, Hong Kong SAR, China
[5]Department of Meteorology and Atmospheric Science, Pennsylvania State University, University Park, PA, USA.

Abstract

Lightning plays a major role in tropospheric oxidation, and its role on modulating tropospheric chemistry was thought to be emissions of nitrogen oxides (NO_x). Recent field and laboratory measurements demonstrate that lightning generates extremely large amounts of oxidants, including hydrogen oxides (HO_x) and O_3. Here we implement these lightning-produced oxidants in a global chemical transport model to examine its global impact on tropospheric composition. We find that lightning-produced oxidants can increase global mass weighted OH by 0.3-10%, and affect CO, O_3, and reactive nitrogen substantially, depending on the emission strength of oxidants from lightning. Our work highlights the importance and uncertainties of lightning-produced oxidants, as well as the need for rethinking the role of lightning in tropospheric oxidation chemistry.

1. Introduction

Lightning plays a major role in tropospheric oxidation chemistry [*Murray et al.*, 2013]. It can produce nitrogen oxides, hydrogen oxides, and ozone through electrical discharges in the atmosphere. Electric discharges in gases have three regions, the dark discharge, glow discharge and arc discharge, with voltage building up during the first two regions before suddenly dropping during the last region because of neutralization (https://en.wikipedia.org/wiki/Electric_discharge_in_gases). We refer these three regions respectively as the subvisible discharge, corona discharge, and flash discharge for atmospheric lightning in this work.

The production of NO by lightning is mainly through the Zel'dovich mechanism during a flash discharge:

$$O_2 + M \longrightarrow O + O + M \quad \text{(R1)}$$

$$O + N_2 \longrightarrow NO + N \quad \text{(R2)}$$

$$N + O_2 \longrightarrow NO + O \quad \text{(R3)}$$

where M = O_2 or N_2. One result of flash discharge is the ohmic heating of ambient air in the vicinity, which increases the temperature over 3000 K within microseconds [*Goldenbaum & Dickerson*, 1993; *Stark et al.*, 1996]. This high ambient temperature largely facilitates reaction (R2), the rate-limiting step in the Zel'dovich mechanism. As such, the flash discharge is referred to as the "hot channel".

In contrast, the production of O_3 and HO_x by lightning does not require high temperatures and have been found in corona discharges and subvisible discharges [*Hill et al.*, 1988; *Jenkins et al.*, 2021]. The production of O_3 by corona discharges is as follows [*Eliasson et al.*, 1987]:

$O_2 + e \longrightarrow O + O + e$ (R4)

$O + O_2 + M \longrightarrow O_3 + M$ (R5)

where e is an electron. We note that for (R1), O atom is produced from O_2 dissociation at high temperature, while for (R4), O atom is produced by the electron attack.

Similar to O_3, the production of HO_x is initiated by the attack of electrons and dissociation of H_2O molecules [*Ershov & Borysow*, 1995; *Gentile & Kushner*, 1995]:

$H_2O + e \longrightarrow H + OH + e$ (R6)

$H + O_2 \longrightarrow HO_2$ (R7)

The production of O_3 and HO_x are further complicated by the production of other species, such as $O(^1D)$ and excited states of N_2 and O_2 [*Eliasson et al.*, 1987; *Lowke & Morrow*, 1995]. The detailed chemistry remains unclear but these mechanisms for production of O_3, OH, and HO_2 are supported by extensive laboratory and field measurements [e.g. *Brune et al.*, 2021; *Jenkins et al.*, 2021].

The role of lightning on modulating global oxidation was mainly considered through emissions of nitrogen oxides (NO_x) from flash discharges [*Chameides et al.*, 1977; *Murray et al.*, 2012], which leads to the production of the major tropospheric oxidants, OH and ozone. The global lightning NO_x (LNO_x) emission is estimated to be about 2-8 Tg N/yr [*Schumann & Huntrieser*, 2007]. The lightning production of hydrogen oxides (LHO_x) was considered unimportant due to their short lifetimes [*Bhetanabhotla et al.*, 1985; *Hill & Rinker*, 1981]. Recent studies show that extremely high amounts of HO_x can be produced by visible flashes and subvisible charges in electrified storms [*Brune et al.*, 2021; *Jenkins et al.*, 2021]. The lightning production of O_3 (LO_3) is shown in the laboratory to occur by corona discharges in higher amounts than LNO_x by a factor of 5-30 on a molar basis [*Hill et al.*, 1988; *Peyrous & Lapeyre*, 1982; *Simek & Clupek*, 2002], but lower production of O_3 was found in flash discharges [*Wang et al.*, 1998]. LO_3 by corona discharges is further supported by field measurements [*Bharali et al.*, 2015; *Bozem et al.*, 2014; *Kotsakis et al.*, 2017; *Minschwaner et al.*, 2008].

Here we implement a simplistic parameterization for lightning HO_x and O_3 into a global chemical transport model (GEOS-Chem) to investigate the global impact of this underappreciated oxidant source (LHO_x and LO_3). Given the large uncertainties associated with current estimates of LHO_x and LO_3, we only focus on their potential global impact in this work.

2. Methods

GEOS-Chem is a global chemical transport model with transport driven by assimilated meteorological fields from the Goddard Earth Observation System (GEOS) of the NASA Global Modeling and Assimilation Office (GMAO) [*Bey et al.*, 2001]. We use GEOS-Chem v12.5.0 (10.5281/zenodo.3403111) to simulate the impact of global lightning-produced oxidants. We use the Modern-Era Retrospective analysis for Research and Applications, version 2 (MERRA-2) reanalysis data from the GEOS archive, which has 3 h temporal resolution (1 h for surface variables and mixing depths) with 0.5° × 0.667° horizontal resolution and 72 vertical layers from the surface to 0.01 hPa. We regrid the meteorological data to a horizontal resolution of 4° latitude ×5° longitude for input to GEOS-Chem.

We configure GEOS-Chem simulations in this work to have fully coupled O_3-NO_x-HO_x-VOC-aerosol chemistry only in the troposphere ("tropchem" mechanism) [*Mao et al.*, 2010, 2013a; *Park et al.*, 2004]. This version includes aerosol reactive uptake of NO_2, NO_3 and N_2O_5, and HO_2 [*Evans & Jacob*, 2005; *Mao et al.*, 2013b, 2013a]. The stratosphere chemistry is represented by a linearized ozone (Linoz) algorithm for ozone [*McLinden et al.*, 2000] and monthly mean sources and loss rate constants for other gases [*Murray et al.*, 2013]. Methane is prescribed with monthly maps of spatially-interpolated NOAA flask data for surface boundary conditions, but is allowed to advect and react [*Murray*, 2016].

The lighting NO_x in GEOS-Chem largely follows Murray et al. [2012], with lightning flash densities and convective cloud depths calculated at the native GEOS-FP meteorology resolution. The simulated climatology is further constrained by the satellite observations from the Optical Transient Detector (OTD) and Lightning Imaging Sensor (LIS), with an annual mean global flash rate of 46 flashes per second [*Cecil et al.*, 2014]. GEOS-Chem applies 500 mol N per flash for all lightning in the northern extratropics (north of 35°N), and 260 mol N per flash for the rest of the world. This approach results in a total lightning emission of 6 Tg N per year. The vertical distribution of lightning follows Ott et al. [2010], which redistributes lightning emissions vertically based on different surface types (tropical continental, tropical marine, subtropical and mid-latitude). It is worth noting that these vertical profiles release the majority of LNO_x in the middle and upper troposphere (Figure S1).

We scale lightning HO_x and O_3 with lightning NO_x by a factor of 10 and 100, to examine its global impact. Our estimated lightning HO_x is based on the following. The OH generated by LHO_x in each electrically active convective cell is estimated to be $3.1\times10^{25} - 2.7\times10^{26}$ molecules per second [*Brune et al.*, 2021]. Assuming globally there are 1800 electrically active convective cells every second [*Schumann & Huntrieser*, 2007], the global production is 3-30 T mol OH/yr. As global lightning NO_x is about 6 Tg N/yr (0.4 T mol N/yr) [*Mao et al.*, 2009; *Travis et al.*, 2020][*Murray*, 2016], we scale lightning HO_x by a factor of 20 and 200 on a molar basis. The scaling of O_3 is based on the estimate from previous studies. The O_3 production rate was estimated to be $0.4 - 98 \times10^{27}$ molecules per flash [*Bozem et al.*, 2014; *Kotsakis et al.*, 2017; *Minschwaner et al.*, 2008], while the NO_x production rate was estimated to be one or two orders of magnitude lower than that of O_3, with $2 - 40 \times10^{25}$ molecules per flash [*Schumann & Huntrieser*, 2007]. We note that the resulting LO_3 is in the range of 140-1400 Tg O_3/yr, comparable to stratosphere-troposphere exchange (STE) ozone flux [*Archibald et al.*, 2020; *Griffiths et al.*, 2021].

Large production of LO_3 is further supported by DC3 field measurements. We estimate LO_3/LHO_x by examining relative enhancement of O_3 to HO_x, for enhanced LHO_x peaks greater than 200 pptv within the past second during DC3 flights, the criteria used in Brune et al. [2021]. These criteria were chosen so that LHO_x was close to its initial value, reducing the possibility that the LO_3/LHO_x ratio was inflated because HO_x, with its short lifetime, had reacted away. Changes in O_3 that corresponded to the LHO_x peaks were then determined. These changes ranged from 0 ppbv for several cases to as more than 60 ppbv, with typical values less than 10 ppbv. The mean value for LO_3/LHO_x (in pptv/pptv) was 15, but it is uncertain by more than a factor of 10 (Table S1). The uncertainty in LO_3/LHO_x is large for four reasons. First, the data set

is limited and may not be representative of the combination of subvisible, corona, and flash discharges occurring in typical thunderstorm anvils. Second, some of the O_3 changes coincident with the LHO_x peaks could be due to other causes of O_3 variability, such as mixing. Third, the observed LHO_x values may be slightly lower than the initial values, which would inflate the ratio. Fourth, the 1-Hz O_3 measurement reduced the actual O_3 peak values of some peaks that were observed to be sub-second wide by the faster 5-Hz HO_x measurement, which would decrease the ratio of LO_3/LHO_x.

We add lightning HO_x and O_3 in a similar fashion as lightning NO_x in the model. As GEOS-Chem is run with operator splitting, we allow radicals (OH + HO_2) and O_3 to accumulate over the course of the emission step (20 mins in our model setup), which leads to a pulse of HO_x radicals at the beginning of the chemistry timestep (also 20 mins). We find in our current model setup that at the end of the emission timestep, OH and HO_2 are built up to the order of ~10^8 molecules/cm^3, an order of magnitude smaller than observed [*Brune et al., 2021*]. The observed values are the peak HO_x concentrations from a single lightning flash in a very small volume ($1x10^{17}$ cm^3 for a typical convective cell) and in a short time period (decay to ambient level within a few seconds), while the model value in a grid box is the sum of numerous flashes in a much larger volume (400 km × 500 km × 1 km = 2×10^{20} cm^3) and accumulated for a much longer time (1200 seconds). As a result, observations and model show similar magnitude on initial HO_x values from lightning. Once the chemistry time step starts, the spikes of OH and HO_2 rapidly decrease due to the dominant loss of radicals through the OH+HO_2 reaction, similar to the box model simulations of HO_x produced from lightning [*Brune et al.*, 2021]. Within seconds, the radical levels return to background levels, while their impact on OH reactants (CO, CH_4) can be significant due to high levels of OH exposure. We consider this treatment a better representation of the impact of lightning, rather than assuming a constant radical source throughout the whole chemistry time step, in which case the OH+HO_2 reaction would be much less of a HO_x sink. In contrast, treating lightning O_3 production as a pulse or time averaged production should not make much difference on ozone, as the lifetime of ozone is on the order of months in the middle and upper troposphere.

We conducted five model simulations for the year of 2016, as illustrated in Table 1. All sensitivity model simulations are initialized with 1 month spin up after 1 year spin up for the base run.

Table 1. Model set up for base run and sensitivity tests

Model run	Lightning emissions	Magnitude (molar basis)
Base	LNO_x	
H10	LNO_x + LHO_x	LOH=10×LNO_x, LHO_2=10×LNO_x
H100	LNO_x + LHO_x	LOH=100×LNO_x, LHO_2=100×LNO_x
H10_O10	LNO_x + LHO_x + LO_3	LOH=10×LNO_x, LHO_2=10×LNO_x, LO_3=10×LNO_x
H100_O100	LNO_x + LHO_x + LO_3	LOH=100×LNO_x, LHO_2=100×LNO_x, LO_3=100×LNO_x

3. Results

Figure 1 shows the global impact of lighting produced oxidants on annual ozone in the upper troposphere. We find that adding LHO_x alone (H10 and H100) will reduce ozone concentrations

in the middle and upper troposphere, due to enhanced ozone loss through $OH/HO_2 + O_3$ as well as reduced ozone production efficiency through $OH + NO_2$ [*Hu et al.*, 2017]. For the case of H10, we find that LHO_x decreases O_3 in the upper troposphere by 1-2 ppbv on an annual mean basis, mainly over regions where lightning flashes are intense. For the run of H100, O_3 can be reduced by 3-7 ppbv in the upper troposphere (Figure S2).

The O_3 decrease due to LHO_x can be compensated by the addition of LO_3. We show in Figure 1 that with the case of H10_O10, annual mean O_3 is in fact enhanced by 1-3 ppbv in the upper troposphere. For the case of H100_O100, annual mean O_3 is enhanced by 10-30 ppbv mainly over lightning-intense regions (Figures 1 and S2). As the O_3 lifetime is on the order of ~1 month, LO_3 can effectively increase ozone in the middle and upper troposphere.

LO_3 improves modeled ozone in free troposphere, although the exact magnitude and spatial variability remains largely uncertain. Figure S4 shows comparison on annual mean vertical profile of ozone mixing ratios in six zonal bands between ozonesonde observations and three model simulations (Base run, H10_O10 and H100_O100) for the year of 2016. The ozonesonde observations are obtained from the World Ozone and Ultraviolet Data Center (WOUDC, http://www.woudc.org), with data only from Electrochemical Concentration Cell (ECC) and no WOUDC-suggested correction factors applied [*Wang et al.*, 2021]. We show that the Base run tends to underestimate ozone in free troposphere by 3-10 ppbv in northern hemisphere (90-60°N, 60-30°N and 30°N-Eq). In fact, this underestimate is even more severe in recent versions of GEOS-Chem with a low bias over 10 ppbv in northern hemisphere, as a result of NO_y reactive uptake by clouds and other updates [*Holmes et al.*, 2019; *Wang et al.*, 2021]. While H10_O10 makes little difference on ozone in free troposphere, we find in Figures S4 that the H100_O100 run overestimates ozone in Northern extratropics and equatorial regions, suggesting the possible magnitude of LO_3 lying between 10 and 100 times of LNO_x. Further refinement of LO_3 requires a comprehensive evaluation of model chemical mechanisms including cloud chemistry and halogen chemistry[*Holmes et al.*, 2019; *Wang et al.*, 2021].

Lightning-produced O_3 offers an alternative explanation to ozone layering in the free troposphere. Atmospheric observations often show layers of high O_3 with high moisture [*Newell et al.*, 1999; *Oltmans et al.*, 1996], and these ozone layers are unlikely to be from stratospheric intrusion because of the high moisture. On the other hand, if these O_3 layer are produced during lightning, they can be transported thousands of kilometers away from the source region because the O_3 lifetime in the upper troposphere is about a month. Lightning-produced O_3 is also consistent with the seasonality of ozone layering, which shows a summer maximum in northern mid-latitudes [*Colette & Ancellet*, 2005].

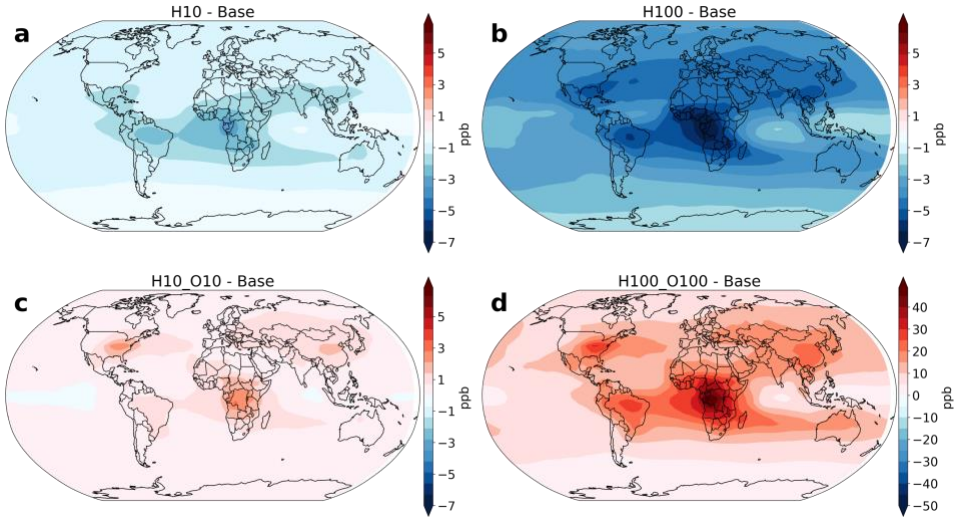

Figure 1 Global impact of lightning oxidants on annual mean O_3 in the upper troposphere (8 km or 350 hPa). Each panel represents the difference between a sensitivity run and base model run: (a) H10 – Base (b) H100 – Base (c) H10_O10 – Base (d) H100_O100 – Base. H10 and H100 are referred to the runs with LHO_x, and H10_O10 and H100_100 are referred to the runs with LHO_x and LO_3 (see Table 1 for details).

Figure 2 shows the impact of lightning oxidants on OH, HO_2, and CO. We note that both H100 and H100_O100 increases OH in the upper troposphere by up to 10% (Figure S2 for zonal mean). The increase of OH is mainly due to the decrease of CO, which allows OH to reach another steady state with higher concentrations, as CO accounts for 40-50% loss of ambient OH [*Mao et al.*, 2009; *Travis et al.*, 2020]. The increase of HO_2 is in part due to direct emission and in part due to OH+CO. We see a mild decease of CO with H10 and H10_O10, but a much bigger decrease with H100 and H100_O100.

We emphasize that the decrease of CO is a result of high levels of OH exposure from lightning-produced HO_x. Despite the majority of HO_x being lost through $OH+HO_2$ in the first few seconds [*Brune et al.*, 2021], CO, CH_4 and other OH reactants are consumed at much higher rate before HO_x returns to ambient level. This additional consumption of CO and other OH reactants by "pulses" of LHO_x, represents the additional oxidative capacity in the atmosphere that is not included in the current estimate of global HO_x budget. As HO_x pulses return to ambient level within a few seconds, these additional radical sources may not be detectable in ambient HO_x measurements outside of electrified clouds.

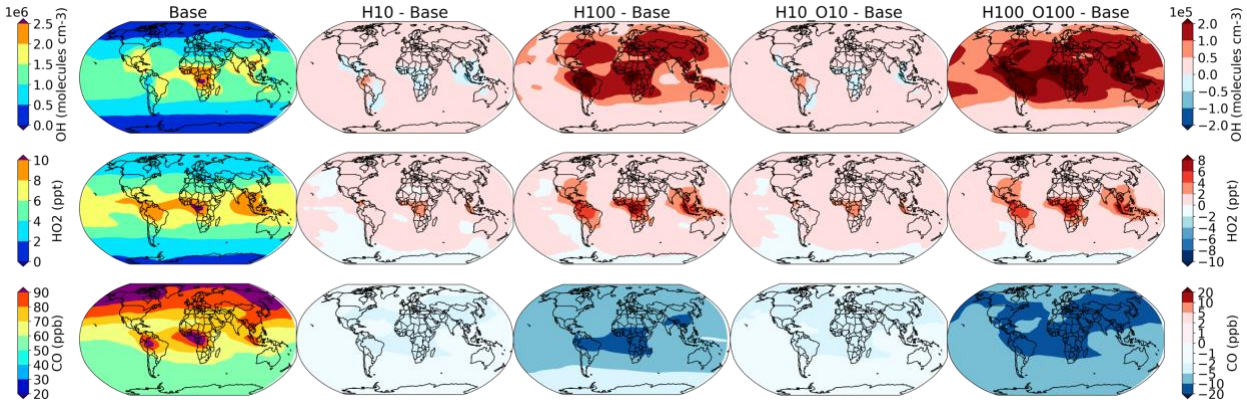

Figure 2 Effect of lightning-produced oxidants on OH (top), HO_2 (middle), and CO (bottom) in the upper troposphere (8 km or 350 hPa). Annual mean results from a simulation for the year of 2016 with the first column as the base model run, and the rest of the columns for the difference between a sensitivity run (H10, H100, O10, O100) and the base run. H10 and H100 are referred to as the runs with LHO_x, and H10_O10 and H100_100 are referred to as the runs with LHO_x and LO_3 (see Table 1 for details).

Table 2 summarizes the global impact of different sensitivity runs. In the base run, global OH production and loss are 220 T mol/yr, in agreement with other model studies [*Lelieveld et al.*, 2016]. The imbalance between Prod(OH) and Loss(OH) in sensitivity runs (H_10, H_100, H10_O10, and H100_O100) reflects the added oxidants (OH, HO_2 and O_3) from lightning before the chemistry timestep. We show that mass-weight global mean OH increases by 0.3%, 3%, 0.8% and 9% with H_10, H_100, H10_O10, and H100_O100 respectively, with little difference on the OH Northern hemisphere to Southern hemisphere ratio. This is expected as the majority of OH burden resides in the tropics [*Naik et al.*, 2013], and impact on OH appears to be mainly in the same region (Figure S2). We note that the impact on global mean OH is smaller than previously estimated by Brune et al. [2021], likely due to two reasons. First, the estimate by Brune et al. [2021] is the direct impact on instantaneous global OH, i.e., a snapshot of the global OH field with pulses from LHO_x included, while our calculation is based on the OH concentrations after chemistry timestep (20 min), during which HO_x pulses decay to background levels within the first few seconds. The impact on global OH from our estimate is mainly resulting from changes on the burden of OH sources and sinks, such as O_3 and CO. Second, the global mass-weighted OH is weighted towards the lower troposphere [*Naik et al.*, 2013], while LHO_x in our model is mainly distributed into the middle and upper troposphere. As a result, the global mass-weighted OH is relatively insensitive to the changes of OH field in the middle and upper troposphere

Lightning-produced oxidants also impact the global CH_4 budget. We find in Table 2 that the global loss of CH_4 increases by 15-110 Tg CH_4/yr from our sensitivity runs. As CH_4 oxidation is rather slow in the upper troposphere, we find that the impact on CH_4 is mainly in the lower troposphere where the potential for LHO_x generation is currently unknown.

Table 2 Global impact of lighting produced oxidants on tropospheric composition

	Base	H10	H100	H10_O10	H100_O100

Global mass-weighted OH (10^6 molecules/cm^3)	1.212	1.216	1.252	1.222	1.324
OH NH/SH ratio	1.21	1.21	1.22	1.21	1.23
Prod Ox (Tg/yr)	5027	5058	5088	4983	4450
Loss Ox (Tg/yr)	4763	4804	4871	4918	6115
Prod OH (Tmol/yr)	222.1	223.8	230.4	225.5	249.8
Loss OH (Tmol/yr)	222.1	228.1	274.1	229.9	293.5
Prod CO (Tmol/yr)	57.2	58.0	61.3	58.2	63.5
Loss CO (Tmol/yr)	87.6	88.7	93.0	88.9	95.4
Loss CH_4 (Tg CH_4/yr)	564.8	579.2	633.6	582.4	676.8
Prod HNO_3 (Tmol/yr)	3.81	3.84	3.93	3.84	3.95
Prod HNO_2 (Tmol/yr)	1.41	1.35	1.36	1.31	1.11
Loss HNO_2 (Tmol/yr)	1.41	1.35	1.36	1.31	1.11

Figure 3 shows the global impact of lighting produced oxidants on the partitioning of reactive nitrogen in the upper troposphere. With newly added OH and HO_2 produced by lightning, $OH+NO_2$ is thus enhanced in the middle and upper troposphere, leading to a higher production of HNO_3 and lower ozone production efficiency (Table 2). We find that both NO and NO_2 in the upper troposphere decreased by 10-20 pptv on an annual mean basis over the tropics and subtropics where lightning activity is high (Figure S3 for zonal mean). In the meantime, we see an increase in most nitrogen reservoirs including HNO_3, peroxyacetyl nitrate (PAN) and peroxynitric acid (HNO_4). The only exception is PAN in H100 and H100_O100, likely due to enhanced loss of PAN through its reaction with OH. This shift of NOx towards their reservoirs may have important implication on nitrogen chemistry in the upper troposphere.

Our results in this work are mainly based on the annual mean, and we expect the impact on shorter time scales to be different. For example, we expect a significant increase of HONO on a short time scale (on the order of hours to days) due to the production of OH and NO as shown in box model simulations [*Brune et al.*, 2021]. Once HONO is photolyzed and returns OH and NO, enhanced OH will lead to higher peroxy radicals that then convert NO_2 to peroxy nitrates and other nitrogen reservoirs, resulting in lower concentrations of NO and NO_2. Consequently, we see a decrease of annual mean HONO production and loss in sensitivity runs in Table 2.

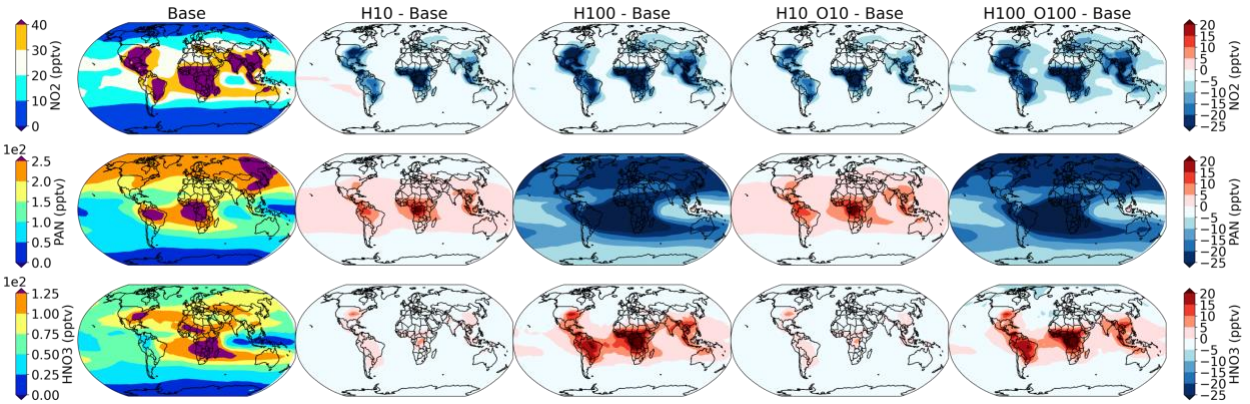

Figure 3 Effect of lightning-produced oxidants on NO_2 (top), PAN (middle), and HNO_3 (bottom) in the upper troposphere (8 km or 350 hPa). Annual mean results from a simulation for the year of 2016 with the first column as base model run, and the rest of the columns showing the difference between a sensitivity run (H10, H100, O10, O100) and the base run. H10 and H100 are referred to as the runs with LHO_x, and H10_O10 and H100_100 are referred to as the runs with LHO_x and LO_3 (see Table 1 for details).

4. Discussion

Here we implement a new source of oxidants ($OH + HO_2 + O_3$) from lighting into a global chemical transport model, to examine its potential impact on tropospheric chemistry. Due to large uncertainties associated with lightning and its emissions, we conduct only a few sensitivity tests to provide a qualitative assessment. However, we find that this additional source of oxidants can increase global mass weighted OH by 0.3-10%, and affect CO, O_3 CH_4 and reactive nitrogen substantially, depending on the emission strength of oxidants from lightning (Table 2).

Large uncertainties remain in many aspects. First, we assume that lightning NO_x and oxidants are instantly mixed in each model grid box when there is lightning. In fact, field observations suggest that NO_x, HO_x, and ozone are likely produced in different parts of storm clouds (NO_x dominates in visible flashes, HO_x and O_3 dominates in subvisible discharges and coronas) [*Jenkins et al.*, 2021; *Brune et al.*, 2021]. It remains unclear how this instant mixing would affect the non-linear behavior of HO_x-NO_x-O_3 chemistry and its possible consequence[*Gressent et al.*, 2016]. Second, the volume of a model grid box in the upper troposphere (approximately 400 km × 500 km × 1 km) is about 1000 times bigger than the typical lightning mapping array (LMA) volume for one convective cell ($1x10^{17}$ cm^3) [*Brune et al.*, 2021], leading to a dilution effect on radical loss through $OH + HO_2$. However, there are typically many electrically active convective cells occupying one model grid box, so the grid box might be only 100 to 1000 times larger than the volume of all the convection within that cell. Also, the fact that we allow the model to build up radicals over the emission timestep (20 mins or 1200 seconds) can somewhat compensate this dilution effect (Figure 4). These effects also imply that our model results may vary with model resolution and the choice of emission timesteps.

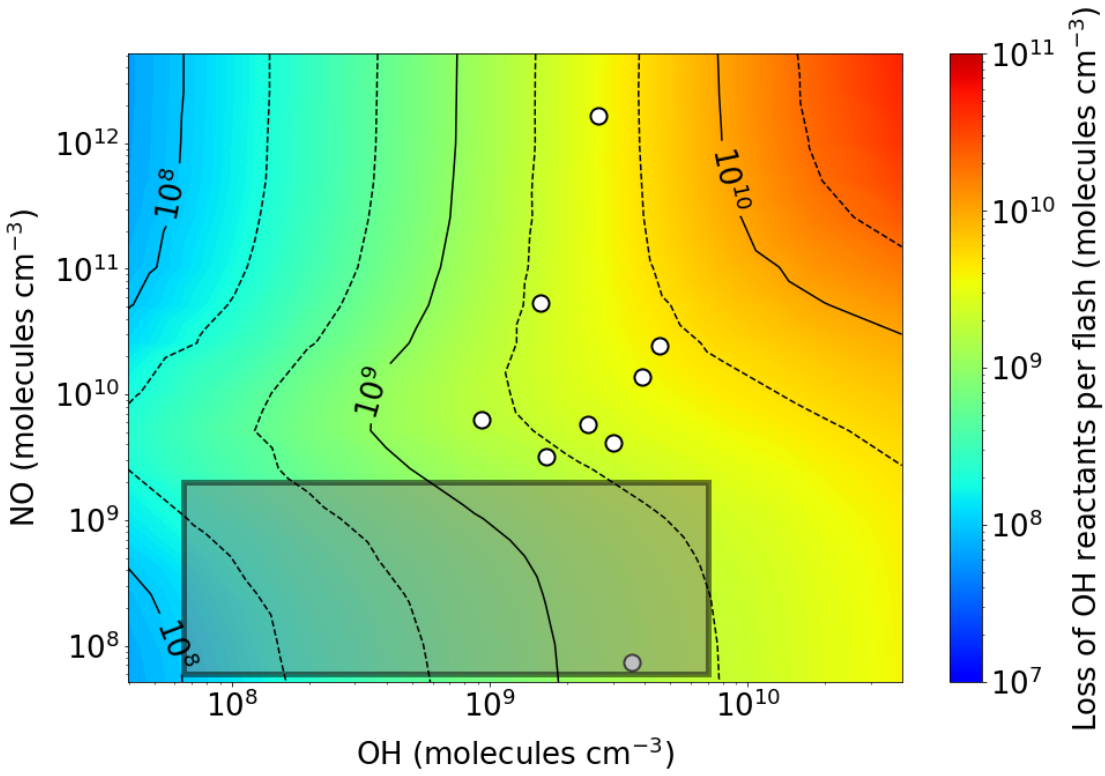

Figure 4 OH loss per flash through reactions with all OH reactants (excluding HO_2 and NO_2), calculated by a box model [*Brune et al.*, 2021]. We exclude HO_2 and NO_2 because their reactions with OH are considered permanent HO_x sinks. The white dots represent the observations from the DC3 aircraft campaign, and the gray box represents the range of model values in the upper troposphere after the emission timestep but before the chemistry timestep.

Our results are further complicated by several aspects of non-linear HO_x-NO_x-O_3 chemistry. One is through the interaction between OH and NO. We show in Figure 4 that the extent of OH loss through reactants other than HO_2 and NO_2, is largely dependent on the relative concentrations of OH and NO. In fact, NO could effectively extend OH lifetimes by producing HONO and reducing OH loss through OH+HO_2 in the first few seconds. As HONO photolyzes and returns OH, OH+HO_2 becomes a minor loss for OH. As shown in Figure 4, the high concentrations of observed NO_x from lightning are not reproduced in the global model, in part due to instant mixing, leading to a lower fraction of OH loss through CO and other OH reactants.

Another aspect is the interaction between NO and O_3. With simultaneous production of NO and O_3, NO+O_3 will convert NO into NO_2 and reduce NO_x lifetime and transport efficiency out of the convective systems and thus impact longer time scale production of OH in the outflow. This non-linear chemistry is therefore sensitive to co-location of LHO_x, LNO_x and LO_3, as well as model configurations and presence of sunlight.

Our work suggests the strong need of revisiting current estimates of global lightning NO_x emissions, with newly added HO_x and O_3. On one hand, OH and HO_2 may further shorten NO_x lifetimes in the upper troposphere (Figure 2 and 3), pointing to a higher level of global LNO_x

[*Nault et al.*, 2017; *Pollack et al.*, 2016]. On the other hand, LO_3 offers an additional source for ozone in the free troposphere, indicating a need for reducing lightning NO_x emissions [*Sauvage et al.*, 2007]. In addition, we show that the nitrogen partitioning is indeed sensitive to lightning-produced oxidants (Figure 3). The role of lightning in tropospheric chemistry may be redefined when LNO_x, LHO_x, and LO_3 are all taken into account, with important implications on global O_3 budget [*Wang et al.*, 2021]. Our work highlights the new challenge of optimizing lightning-produced NO, HO_x, and O_3 emissions in a holistic way for future lightning-related research.

Acknowledgement

J. Mao acknowledges GEOS-Chem supporting team for help. J. Mao and T. Zhao acknowledge the support from NASA grant 80NSSC21K0428, 80NSSC19M0154 and NSF grant AGS-2026821. W. Brune acknowledges support from NSF AGS-1834711 and NASA NNX12AB84G. We thank Jeff Peischl, Ilana Pollack and Thomas Ryerson, for the use of their measurements from DC3 aircraft campaign. We thank Dr. Lee T. Murray and another reviewer for their insightful comments on an early version of the draft.

Data Availability Statement

The model output for both base run and sensitivity runs can be accessed online (at Dryad, the link is private and data will be public once paper is accepted https://datadryad.org/stash/share/HfAiiT8arepmIaRPR7TUDQYmiLWVLr1X0_KzCtRU3p0).

Reference

Archibald, A. T., Neu, J. L., Elshorbany, Y. F., Cooper, O. R., Young, P. J., Akiyoshi, H., et al. (2020). Tropospheric Ozone Assessment Report: A critical review of changes in the tropospheric ozone burden and budget from 1850 to 2100. *Elementa: Science of the Anthropocene*, *8*(1). https://doi.org/10.1525/elementa.2020.034

Bey, I., Jacob, D. J., Yantosca, R. M., Logan, J. A., Field, B. D., Fiore, A. M., et al. (2001). Global modeling of tropospheric chemistry with assimilated meteorology: Model description and evaluation. *Journal of Geophysical Research-Atmospheres*, *106*(D19), 23073–23095.

Bharali, C., Pathak, B., & Bhuyan, P. K. (2015). Spring and summer night-time high ozone episodes in the upper Brahmaputra valley of North East India and their association with

lightning. *Atmospheric Environment*, *109*, 234–250. https://doi.org/10.1016/j.atmosenv.2015.03.035

Bhetanabhotla, M. N., Crowell, B. A., Coucouvinos, A., Hill, R. D., & Rinker, R. G. (1985). Simulation of trace species production by lightning and corona discharge in moist air. *Atmospheric Environment (1967)*, *19*(9), 1391–1397. https://doi.org/10.1016/0004-6981(85)90276-8

Bozem, H., Fischer, H., Gurk, C., Schiller, C. L., Parchatka, U., Koenigstedt, R., et al. (2014). Influence of corona discharge on the ozone budget in the tropical free troposphere: a case study of deep convection during GABRIEL. *Atmospheric Chemistry and Physics*, *14*(17), 8917–8931. https://doi.org/10.5194/acp-14-8917-2014

Brune, W. H., McFarland, P. J., Bruning, E., Waugh, S., MacGorman, D., Miller, D. O., et al. (2021). Extreme oxidant amounts produced by lightning in storm clouds. *Science*, *372*(6543), 711–715. https://doi.org/10.1126/science.abg0492

Cecil, D. J., Buechler, D. E., & Blakeslee, R. J. (2014). Gridded lightning climatology from TRMM-LIS and OTD: Dataset description. *Atmospheric Research*, *135–136*, 404–414. https://doi.org/10.1016/j.atmosres.2012.06.028

Chameides, W. L., Stedman, D. H., Dickerson, R. R., Rusch, D. W., & Cicerone, R. J. (1977). NOx Production in Lightning. *Journal of the Atmospheric Sciences*, *34*(1), 143–149. https://doi.org/10.1175/1520-0469(1977)034<0143:NPIL>2.0.CO;2

Colette, A., & Ancellet, G. (2005). Impact of vertical transport processes on the tropospheric ozone layering above Europe.: Part II: Climatological analysis of the past 30 years. *Atmospheric Environment*, *39*(29), 5423–5435. https://doi.org/10.1016/j.atmosenv.2005.06.015

Eliasson, B., Hirth, M., & Kogelschatz, U. (1987). Ozone synthesis from oxygen in dielectric barrier discharges. *Journal of Physics D: Applied Physics*, *20*(11), 1421–1437. https://doi.org/10.1088/0022-3727/20/11/010

Ershov, A., & Borysow, J. (1995). Dynamics of OH (X2Pi , v=0) in high-energy atmospheric pressure electrical pulsed discharge. *Journal of Physics D: Applied Physics*, *28*(1), 68–74. https://doi.org/10.1088/0022-3727/28/1/012

Evans, M. J., & Jacob, D. J. (2005). Impact of new laboratory studies of N2O5 hydrolysis on global model budgets of tropospheric nitrogen oxides, ozone, and OH. *Geophysical Research Letters*, *32*(9). https://doi.org/L09813,10.1029/2005gl022469

Gentile, A. C., & Kushner, M. J. (1995). Reaction chemistry and optimization of plasma remediation of NxOy from gas streams. *Journal of Applied Physics*, *78*(3), 2074–2085. https://doi.org/10.1063/1.360185

Goldenbaum, G. C., & Dickerson, R. R. (1993). Nitric oxide production by lightning discharges. *Journal of Geophysical Research: Atmospheres*, *98*(D10), 18333–18338. https://doi.org/10.1029/93JD01018

Gressent, A., Sauvage, B., Cariolle, D., Evans, M., Leriche, M., Mari, C., & Thouret, V. (2016). Modeling lightning-NO_x chemistry on a sub-grid scale in a global chemical transport model. *Atmospheric Chemistry and Physics*, *16*(9), 5867–5889. https://doi.org/10.5194/acp-16-5867-2016

Griffiths, P. T., Murray, L. T., Zeng, G., Shin, Y. M., Abraham, N. L., Archibald, A. T., et al. (2021). Tropospheric ozone in CMIP6 simulations. *Atmospheric Chemistry and Physics*, *21*(5), 4187–4218. https://doi.org/10.5194/acp-21-4187-2021

Hill, R. D., & Rinker, R. G. (1981). Production of nitrate ions and other trace species by lightning. *Journal of Geophysical Research: Oceans*, *86*(C4), 3203–3209. https://doi.org/10.1029/JC086iC04p03203

Hill, R. D., Rahmim, I., & Rinker, R. G. (1988). Experimental study of the production of nitric oxide, nitrous oxide, and ozone in a simulated atmospheric corona. *Industrial & Engineering Chemistry Research*, *27*(7), 1264–1269. https://doi.org/10.1021/ie00079a029

Holmes, C. D., Bertram, T. H., Confer, K. L., Graham, K. A., Ronan, A. C., Wirks, C. K., & Shah, V. (2019). The Role of Clouds in the Tropospheric NOx Cycle: A New Modeling Approach for Cloud Chemistry and Its Global Implications. *Geophysical Research Letters*, *46*(9), 4980–4990. https://doi.org/10.1029/2019GL081990

Hu, L., Jacob, D. J., Liu, X., Zhang, Y., Zhang, L., Kim, P. S., et al. (2017). Global budget of tropospheric ozone: Evaluating recent model advances with satellite (OMI), aircraft (IAGOS), and ozonesonde observations. *Atmospheric Environment*, *167*, 323–334. https://doi.org/10.1016/j.atmosenv.2017.08.036

Jenkins, J. M., Brune, W. H., & Miller, D. O. (2021). Electrical Discharges Produce Prodigious Amounts of Hydroxyl and Hydroperoxyl Radicals. *Journal of Geophysical Research: Atmospheres*, *126*(9), e2021JD034557. https://doi.org/10.1029/2021JD034557

Kotsakis, A., Morris, G. A., Lefer, B., Jeon, W., Roy, A., Minschwaner, K., et al. (2017). Ozone production by corona discharges during a convective event in DISCOVER-AQ Houston. *Atmospheric Environment*, *161*, 13–17. https://doi.org/10.1016/j.atmosenv.2017.04.018

Lelieveld, J., Gromov, S., Pozzer, A., & Taraborrelli, D. (2016). Global tropospheric hydroxyl distribution, budget and reactivity. *Atmospheric Chemistry and Physics*, *16*(19), 12477–12493. https://doi.org/10.5194/acp-16-12477-2016

Lowke, J. J., & Morrow, R. (1995). Theoretical analysis of removal of oxides of sulphur and nitrogen in pulsed operation of electrostatic precipitators. *IEEE Transactions on Plasma Science*, *23*(4), 661–671. https://doi.org/10.1109/27.467988

Mao, J., Ren, X., Brune, W. H., Olson, J. R., Crawford, J. H., Fried, A., et al. (2009). Airborne measurement of OH reactivity during INTEX-B. *Atmospheric Chemistry and Physics*, *9*(1), 163–173. https://doi.org/10.5194/acp-9-163-2009

Mao, J., Jacob, D. J., Evans, M. J., Olson, J. R., Ren, X., Brune, W. H., et al. (2010). Chemistry of hydrogen oxide radicals (HOx) in the Arctic troposphere in spring. *Atmospheric Chemistry and Physics*, *10*(13), 5823–5838. https://doi.org/10.5194/acp-10-5823-2010

Mao, J., Paulot, F., Jacob, D. J., Cohen, R. C., Crounse, J. D., Wennberg, P. O., et al. (2013a). Ozone and organic nitrates over the eastern United States: Sensitivity to isoprene chemistry. *Journal of Geophysical Research: Atmospheres*, *118*(19), 2013JD020231. https://doi.org/10.1002/jgrd.50817

Mao, J., Fan, S.-M., Jacob, D. J., & Travis, K. R. (2013b). Radical loss in the atmosphere from Cu-Fe redox coupling in aerosols. *Atmospheric Chemistry and Physics*, *13*(2), 509–519. https://doi.org/10.5194/acp-13-509-2013

McLinden, C. A., Olsen, S. C., Hannegan, B., Wild, O., Prather, M. J., & Sundet, J. (2000). Stratospheric ozone in 3-D models: A simple chemistry and the cross-tropopause flux. *Journal of Geophysical Research-Atmospheres*, *105*(D11), 14653–14665.

Minschwaner, K., Kalnajs, L. E., Dubey, M. K., Avallone, L. M., Sawaengphokai, P. C., Edens, H. E., & Winn, W. P. (2008). Observation of enhanced ozone in an electrically active storm over Socorro, NM: Implications for ozone production from corona discharges. *Journal of Geophysical Research: Atmospheres*, *113*(D17). https://doi.org/10.1029/2007JD009500

Murray, L. T. (2016). Lightning NOxand Impacts on Air Quality. *Current Pollution Reports*, *2*(2), 115–133. https://doi.org/10.1007/s40726-016-0031-7

Murray, L. T., Jacob, D. J., Logan, J. A., Hudman, R. C., & Koshak, W. J. (2012). Optimized regional and interannual variability of lightning in a global chemical transport model constrained by LIS/OTD satellite data. *J. Geophys. Res.*, *117*(D20), D20307. https://doi.org/10.1029/2012jd017934

Murray, L. T., Logan, J. A., & Jacob, D. J. (2013). Interannual variability in tropical tropospheric ozone and OH: The role of lightning: IAV IN OZONE AND OH-ROLE OF LIGHTNING. *Journal of Geophysical Research: Atmospheres*, *118*(19), 11,468-11,480. https://doi.org/10.1002/jgrd.50857

Naik, V., Voulgarakis, A., Fiore, A. M., Horowitz, L. W., Lamarque, J. F., Lin, M., et al. (2013). Preindustrial to present-day changes in tropospheric hydroxyl radical and methane lifetime from the Atmospheric Chemistry and Climate Model Intercomparison Project (ACCMIP). *Atmos. Chem. Phys.*, *13*(10), 5277–5298. https://doi.org/10.5194/acp-13-5277-2013

Nault, B. A., Laughner, J. L., Wooldridge, P. J., Crounse, J. D., Dibb, J., Diskin, G., et al. (2017). Lightning NOx Emissions: Reconciling Measured and Modeled Estimates With Updated

NOx Chemistry. *Geophysical Research Letters*, *44*(18), 9479–9488. https://doi.org/10.1002/2017GL074436

Newell, R. E., Thouret, V., Cho, J. Y. N., Stoller, P., Marenco, A., & Smit, H. G. (1999). Ubiquity of quasi-horizontal layers in the troposphere. *Nature*, *398*(6725), 316–319. https://doi.org/10.1038/18642

Oltmans, S. J., Levy, H., Harris, J. M., Merrill, J. T., Moody, J. L., Lathrop, J. A., et al. (1996). Summer and spring ozone profiles over the North Atlantic from ozonesonde measurements. *Journal of Geophysical Research: Atmospheres*, *101*(D22), 29179–29200. https://doi.org/10.1029/96JD01713

Ott, L. E., Pickering, K. E., Stenchikov, G. L., Allen, D. J., DeCaria, A. J., Ridley, B., et al. (2010). Production of lightning NOx and its vertical distribution calculated from three-dimensional cloud-scale chemical transport model simulations. *Journal of Geophysical Research-Atmospheres*, *115*. https://doi.org/10.1029/2009jd011880

Park, R. J., Jacob, D. J., Field, B. D., Yantosca, R. M., & Chin, M. (2004). Natural and transboundary pollution influences on sulfate-nitrate-ammonium aerosols in the United States: Implications for policy. *Journal of Geophysical Research-Atmospheres*, *109*(D15). https://doi.org/D15204,10.1029/2003jd004473

Peyrous, R., & Lapeyre, R.-M. (1982). Gaseous products created by electrical discharges in the atmosphere and condensation nuclei resulting from gaseous phase reactions. *Atmospheric Environment (1967)*, *16*(5), 959–968. https://doi.org/10.1016/0004-6981(82)90182-2

Pollack, I. B., Homeyer, C. R., Ryerson, T. B., Aikin, K. C., Peischl, J., Apel, E. C., et al. (2016). Airborne quantification of upper tropospheric NOx production from lightning in deep

convective storms over the United States Great Plains. *Journal of Geophysical Research: Atmospheres*, *121*(4), 2002–2028. https://doi.org/10.1002/2015JD023941

Sauvage, B., Martin, R. V., van Donkelaar, A., Liu, X., Chance, K., Jaeglé, L., et al. (2007). Remote sensed and in situ constraints on processes affecting tropical tropospheric ozone. *Atmospheric Chemistry and Physics*, *7*(3), 815–838.

Schumann, U., & Huntrieser, H. (2007). The global lightning-induced nitrogen oxides source. *Atmospheric Chemistry and Physics*, *7*(14), 3823–3907. https://doi.org/10.5194/acp-7-3823-2007

Simek, M., & Clupek, M. (2002). Efficiency of ozone production by pulsed positive corona discharge in synthetic air. *Journal of Physics D: Applied Physics*, *35*(11), 1171–1175. https://doi.org/10.1088/0022-3727/35/11/311

Stark, M. S., Harrison, J. T. H., & Anastasi, C. (1996). Formation of nitrogen oxides by electrical discharges and implications for atmospheric lightning. *Journal of Geophysical Research: Atmospheres*, *101*(D3), 6963–6969. https://doi.org/10.1029/95JD03008

Travis, K. R., Heald, C. L., Allen, H. M., Apel, E. C., Arnold, S. R., Blake, D. R., et al. (2020). Constraining remote oxidation capacity with ATom observations. *Atmospheric Chemistry and Physics*, *20*(13), 7753–7781. https://doi.org/10.5194/acp-20-7753-2020

Wang, X., Jacob, D. J., Downs, W., Zhai, S., Zhu, L., Shah, V., et al. (2021). Global tropospheric halogen (Cl, Br, I) chemistry and its impact on oxidants. *Atmospheric Chemistry and Physics Discussions*, 1–34. https://doi.org/10.5194/acp-2021-441

Wang, Y., DeSilva, A. W., Goldenbaum, G. C., & Dickerson, R. R. (1998). Nitric oxide production by simulated lightning: Dependence on current, energy, and pressure. *Journal*

of Geophysical Research: Atmospheres, *103*(D15), 19149–19159.

https://doi.org/10.1029/98JD01356

Supplementary material
for
Global impact of lightning-produced oxidants

Jingqiu Mao[1], Tianlang Zhao[1], Christoph A. Keller[2,3], Xuan Wang[4], Patrick J. McFarland[5], Jena M. Jenkins[5], William H. Brune[7]

[1]Department of Chemistry and Biochemistry and Geophysical Institute, University of Alaska, Fairbanks, Fairbanks, AK, USA.
[2]Universities Space Research Association, Columbia, MD, USA
[3]NASA Global Modeling and Assimilation Office, Goddard Space Flight Center, Greenbelt, MD, USA
[4]School of Energy and Environment, City University of Hong Kong, Hong Kong SAR, China
[5]Department of Meteorology and Atmospheric Science, Pennsylvania State University, University Park, PA, USA.

Table S1 Enhancement of O_3 and HO_x for HO_x peak events during DC-3 flights

Flight date (YYMMDD)	time (hh:mm:ss)	HO_x (pptv)	O_3 (ppbv)	$1000*O_3/HO_x$
120529	23:30:28	730	2	2.7
120616	02:05:40	2000	2.5	1.3
120623	00:07:09	116	4	34.5
120623	00:08:19	250	0	0
120623	00:09:37	450	14	31.1
120623	00:16:21	2000	62	31.0
120623	00:17:08	609	5	8.2
120623	00:36:15	139	3	21.6
120623	00:41:55	426	0	0
120623	00:56:27	1984	31	15.6
120623	01:23:13	210	8	38.1
120623	02:06:25	340	0	0
120623	02:07:56	225	3	13.3
			median	13.3
			mean	15.2

Table S2. Model set up for base run and sensitivity tests

Model run	Lightning emissions	Magnitude (molar basis)
Base	LNO_x	
H10	LNO_x + LHO_x	$LOH=10\times LNO_x$, $LHO_2=10\times LNO_x$
H100	LNO_x + LHO_x	$LOH=100\times LNO_x$, $LHO_2=100\times LNO_x$
H10_O10	LNO_x + LHO_x + LO_3	$LOH=10\times LNO_x$, $LHO_2=10\times LNO_x$, $LO_3=10\times LNO_x$
H100_O100	LNO_x + LHO_x + LO_3	$LOH=100\times LNO_x$, $LHO_2=100\times LNO_x$, $LO_3=100\times LNO_x$

Table S3 Global impact of lighting produced oxidants on tropospheric composition

	Base	H10	H100	H10_O10	H100_O100
Global mass-weighted OH (10^6 molecules/cm^3)	1.212	1.216	1.252	1.222	1.324
OH NH/SH ratio	1.21	1.21	1.22	1.21	1.23
Prod Ox (Tg/yr)	5027	5058	5088	4983	4450
Loss Ox (Tg/yr)	4763	4804	4871	4918	6115
Prod OH (Tmol/yr)	222.1	223.8	230.4	225.5	249.8
Loss OH (Tmol/yr)	222.1	228.1	274.1	229.9	293.5
Prod CO (Tmol/yr)	57.2	58.0	61.3	58.2	63.5
Loss CO (Tmol/yr)	87.6	88.7	93.0	88.9	95.4
Loss CH_4 (Tg CH_4/yr)	564.8	579.2	633.6	582.4	676.8
Prod HNO_3 (Tmol/yr)	3.81	3.84	3.93	3.84	3.95
Prod HNO_2 (Tmol/yr)	1.41	1.35	1.36	1.31	1.11
Loss HNO_2 (Tmol/yr)	1.41	1.35	1.36	1.31	1.11

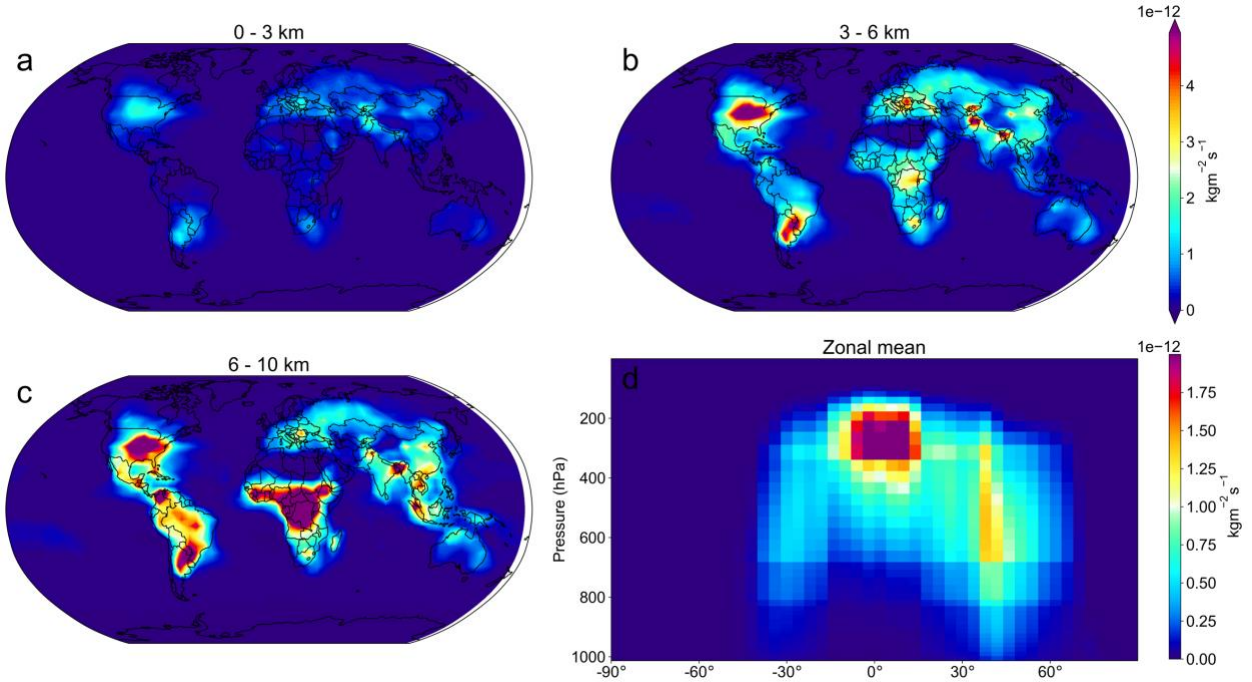

Figure S1. Annual mean global lightning NO emissions for the year of 2016. The total column is averaged for (a) lower troposphere at 0-3 km, (b) middle troposphere at 3-6 km and (c) upper troposphere at 6-10 km. The zonal mean of global lightning NO emissions is shown in (d).

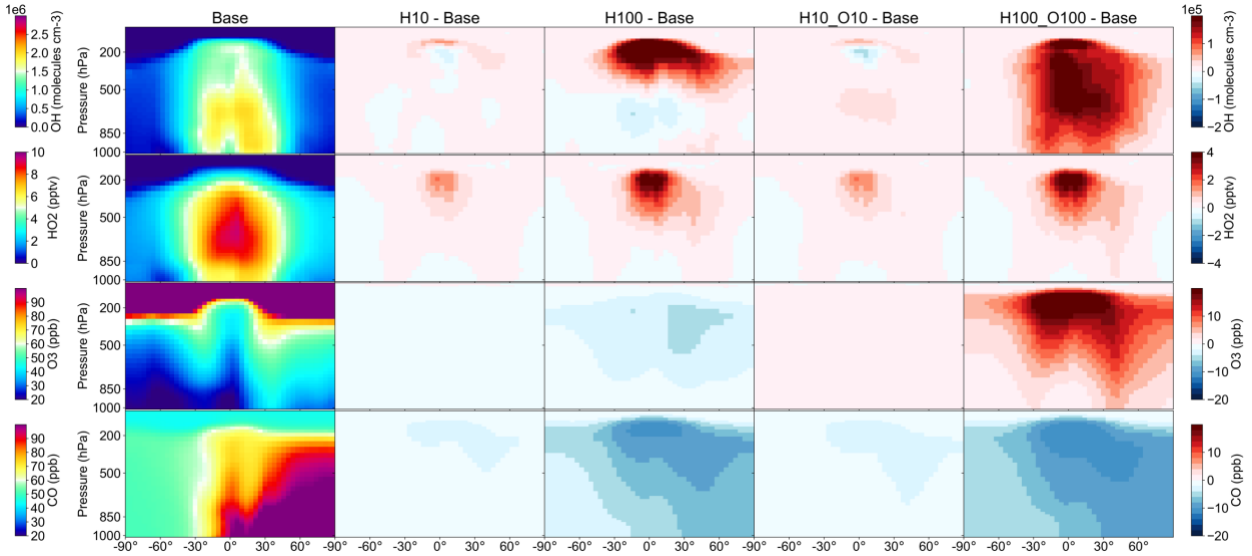

Figure S2. Zonal mean effect of lightning-produced oxidants on OH (top), HO_2 (second row), O_3 (third row) and CO (bottom). Results are from a simulation for the year of 2016 where the first column represents the base model run, and the rest of the columns show the difference between a sensitivity run (H10, H100, O10, O100) and the base run. H10 and H100 are referred to as the runs with LHO_x, and H10_O10 and H100_100 are referred to as the runs with LHO_x and LO_3 (see Table 1 for details).

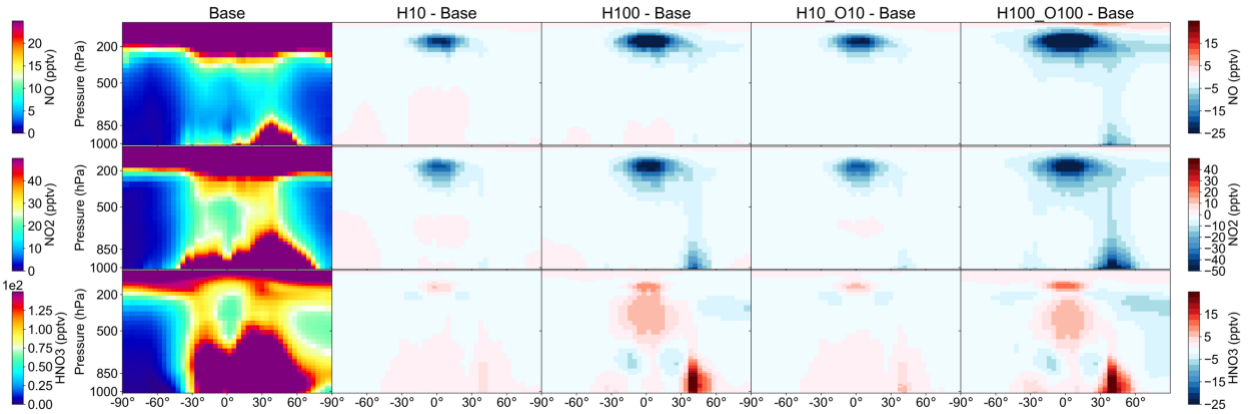

Figure S3. Zonal mean effect of lightning-produced oxidants on NO (top), NO_2 (middle), and HNO_3 (bottom). Results are from a simulation for the year of 2016 where the first column represents the base model run, and the rest of the columns show the difference between a sensitivity run (H10, H100, O10, O100) and the base run. H10 and H100 are referred to as the runs with LHO_x, and H10_O10 and H100_100 are referred to as the runs with LHO_x and LO_3 (see Table 1 for details).

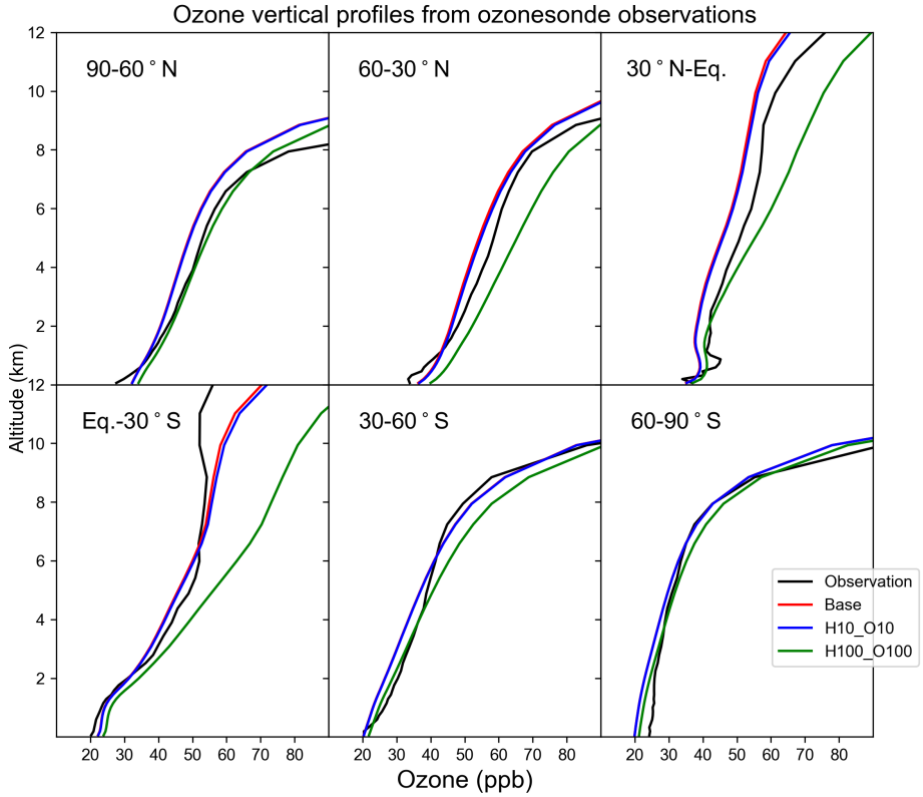

Figures S4. Annual mean vertical profile of ozone mixing ratios in six zonal bands from ozonesonde observations and three model simulations for the year of 2016. The ozonesonde observations are obtained from the World Ozone and Ultraviolet Data Center (WOUDC, http://www.woudc.org). Three model runs (Base, H10_O10 and H100_O100) are from the base model run and two sensitivity runs with details in Table 1.